International Journal of Scientific Engineering and Research (IJSER)
www.ijser.in
ISSN (Online): 2347-3878, Impact Factor (2014): 3.05

Optimization of Bursting Behavior of AA2090 Al-Alloy Pipes Using Taguchi Techniques and Finite Element Analysis

R. Venkata Sai Krishna Varma[1], A. Chennakesava Reddy[2]

[1]UG student, Department of Mechanical Engineering, JNTUH College of Engineering, Hyderabad, India
[2]Professor, Department of Mechanical Engineering, JNTUH College of Engineering, Hyderabad, India

Abstract: ***The optimization of bursting behavior of liquid and gas pipe lines is very important with respect to safety. In this paper 3D finite element analysis and Taguchi technique were employed to investigate fracture criteria of AA2090 Al-alloy pipes subjected to internal bursting pressure. The ultimate tensile strength criterion was employed to study the failure of pipes. The heat treatment was the major dominating control factor effecting the bursting of pipes.***

Keywords: AA2090 Al-alloy, bursting pressure, crack length, crack depth, heat treatment, finite element analysis.

1. Introduction

The pipelines must be monitored continuously and probable problems must be evaluated consistently, to evaluate the structural integrity of the pipe and to repair the pipes safely, before thee defects in them cause an accident. The metal loss due to corrosion defects has become one of the leading causes of pipeline failure. AA2090 is an aluminum-lithium alloy developed for high strength aerospace applications. This Al-alloy offers an 8 per cent density savings when compared with other aerospace alloys. More recently, they have been investigated for use in cryogenic applications. Numerous methods have been developed for predicting the burst pressure of blunt part-wall defects, which characterize the behavior of typical corrosion defects [1, 2, 3, 4]. ASME B31G, DNV-RP-F101, SHELL-92 and RESTRENG were applied to assess the strength of thin tubes [5, 6, 7, 8]. The finite element analysis (FEA) is one of the most efficient tools to quantify reliably the remaining strength of corroded pipes. Elastic-Plastic finite element models have been used to provide more accurate results in evaluating the corrosion defects [9, 10, 11].

The present work was aimed at to evaluate crack propagation and bursting of AA2090 Al-alloy pipes with predefined flaws of varying length and depth using finite element analysis.

Table 1: Control factors and their levels

Factor	*Symbol*	*Level–1*	*Level–2*	*Level–3*
Thickness, mm	A	1.0	1.2	1.5
Length of crack, mm	B	25	50	75
Depth of crack	C	30%t	40%t	50%t
Heat treatment	D	T3	T84	T83

where t is pipe thickness

2. Materials and Methods

The material of pipes was AA2090 Al-alloy. The chosen control parameters are summarized in table 1. The orthogonal array (OA), L9 was selected for the present work. The control factors were assigned to the various columns of O.A. The assignment of control factors along with the OA matrix is given in table 2. The pipe model and surface crack were modeled using computer aided design (CAD) tools [12]. A surface notch made on the outer surface of the pipe specimen. The dimensions of notch are given in figure 1.

Table 2: Orthogonal Array (L9) and control factors

Treat No.	*A*	*B*	*C*	*D*
1	1	1	1	1
2	1	2	2	2
3	1	3	3	3
4	2	1	2	3
5	2	2	3	1
6	2	3	1	2
7	3	1	3	2
8	3	2	1	3
9	3	3	2	1

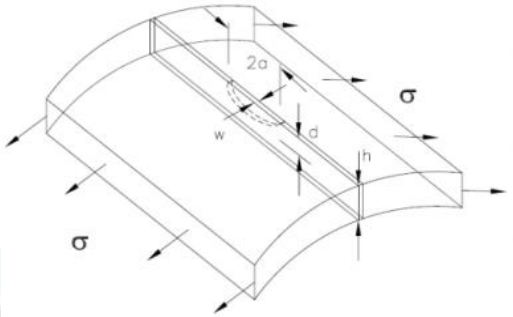

Figure 1: The Crack dimensions.

The operating pressure was obtained from the following expression:

$$P = 0.60\,\sigma_y(2t/D) \times (1 - t/d) \quad (1)$$

where *P* is the design pressure (MPa), σ_y is the yield strength (MPa), t is the nominal wall thickness (mm), D is the nominal outside diameter (mm), and d is the crack depth.

The ANSYS 14.5v code was used to model the pipe and initial semi-elliptical crack. The pipe was meshed with tetrahedron elements. Fracture module method for crack generation required that elements be of higher order. Therefore, out of choice of tetrahedral elements of type SOLID 186 were chosen for accurate results [13]. Fine mesh was used to model the crack region. The number of elements and nodes were

1,78,241 and 3,31,648 respectively. A three-dimensional semi-elliptical crack was initiated on the pipe surface. The crack was oriented with respect to pipe axis as shown in figure 2. The pressure obtained from Eq. (1) was applied on the inner surface of pipe.

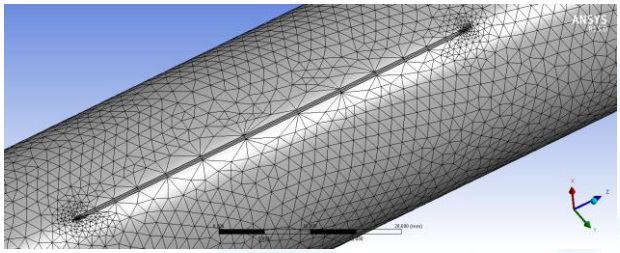

Figure 2: Meshing of crack and pipe.

If the failure is defined by material ultimate tensile strength, it follows that the design goal is to limit the maximum equivalent stress to be less than the ultimate tensile strength of the material:

$$ES/UTS < 1 \quad (2)$$

where, ES is the equivalent stress and UTS is the yield strength of AA2090 Al-alloy.

3. Results and Discussion

The finite element software was carried out twice with two mesh densities according Taguchi design of experimentation.

3.1 Static deformation

Figure 3 gives the total deformation values of tested pipes as per Taguchi experimentation. For the pipes having thickness of 1mm the maximum total deformation of 0.049 mm was observed with test coupon 3 and the minimum total deformation of 0.015 mm test coupon 1. For the pipes having thickness of 1.2 mm the maximum total deformation of 0.041 mm was observed with test coupon 4 and the minimum total deformation of 0.018 mm test coupon 5. For the pipes having thickness of 1.5 mm the maximum total deformation of 0.041 mm was observed with test coupon 7 and the minimum total deformation of 0.017 mm test coupon 9.

3.2 Equivalent stress distribution across the crack

The equivalent stress distribution across the crack for all the test coupons is shown in figure 4. The maximum equivalent stress of test coupons 1, 2, 3, 4, 5, 6, 7, 8 and 9, respectively 327.29 MPa, 713.29 MPa, 1580.00 MPa, 868.42 MPa, 308.08 MPa, 906.24 MPa, 752.88 MPa, 805.03 and 402.44 MPa. The equivalent stresses of test coupons 1, 5 and 9 were belonging to heat treatment, T3. For the test coupon 5only the equivalent stress was not exceeded the ultimate tensile strength (320 MPa) of AA2090 whereas the ultimate tensile strength was exceeded for the test coupons 1 and 8. The equivalent stresses of trials 2, 6 and 7 were belonging to heat treatment, T84. For the entire test coupons the equivalent stress was exceeded the ultimate tensile strength (525 MPa) of AA2090. The equivalent stresses of trials 3, 4 and 8 were belonging to heat treatment, T83. For all test coupons the equivalent stress was exceeded the ultimate tensile strength (550 MPa) of AA2090 alloy.

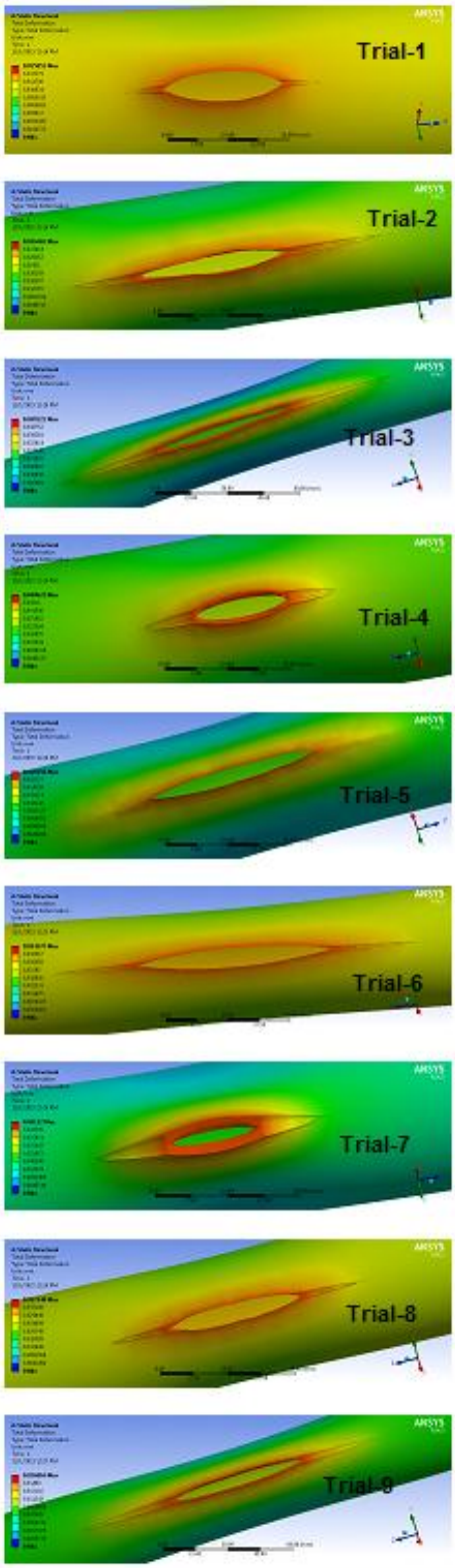

Figure 3: Total deformations of all test coupons.

3.3 J-integral

The path dependence of the J-integral is displayed for all nine test coupons in figure 5. The maximum value of J-integral was 1.5619 MJ/mm^2 with the test coupon 7 having the displacement of 0.041 mm. The minimum value of J-integral was 0.1221 MJ/mm^2 with the test coupon 1 having the displacement of 0.015 mm. Therefore, the J-integral is directly proportional to the displacement of the load applied on the

pipe. The path dependence of the J-integral was much more significant in a large deformation analysis [14].

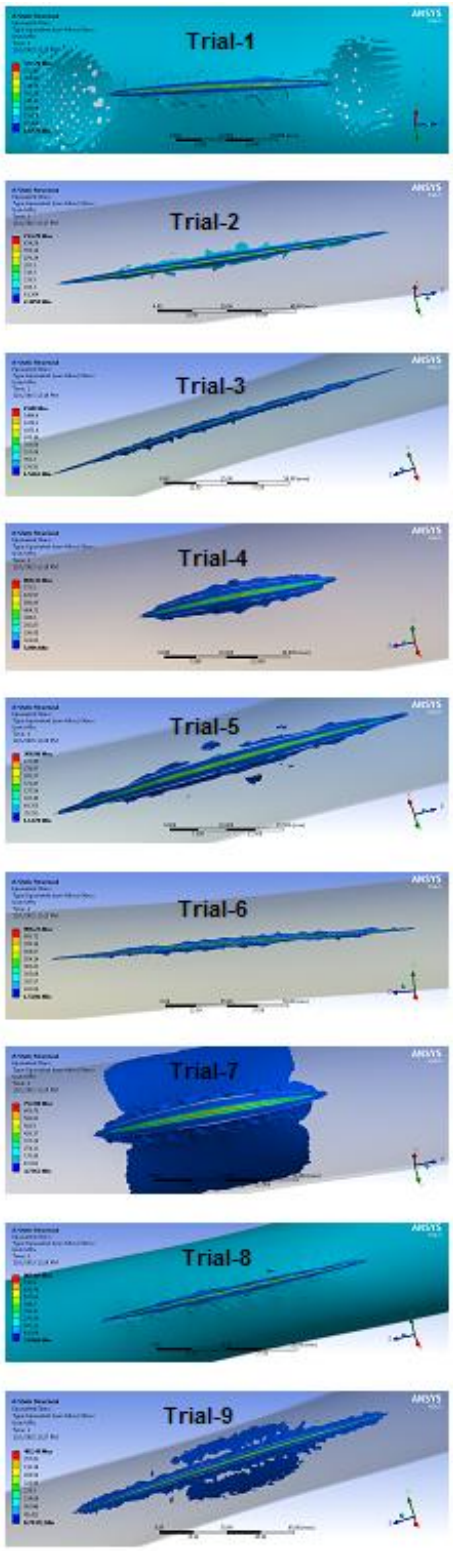

Figure 4: Equivalent stresses of all test coupons.

3.4 Stress Intensity Factors

Figure 6 shows the variations of stress intensity factor, KI along the initial crack-front for all pipes. The stress intensity factors, KII and KIII are not highly influential factors as compared to stress intensity factor KI. The test coupon 7 has the maximum value (365.10) of KI whereas the test coupon 1 has the minimum value (102.49) of KI.

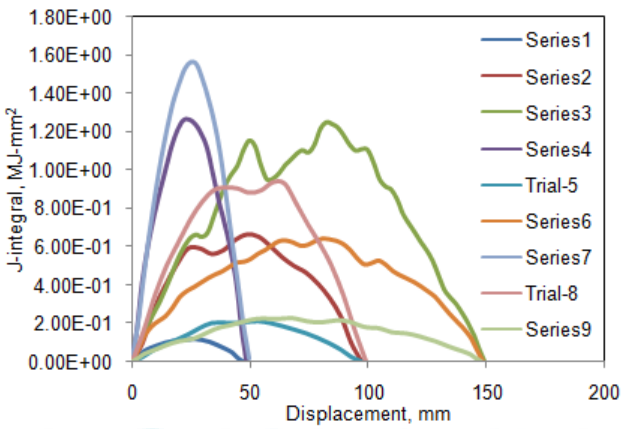

Figure 5: J-Integral values of all test coupons.

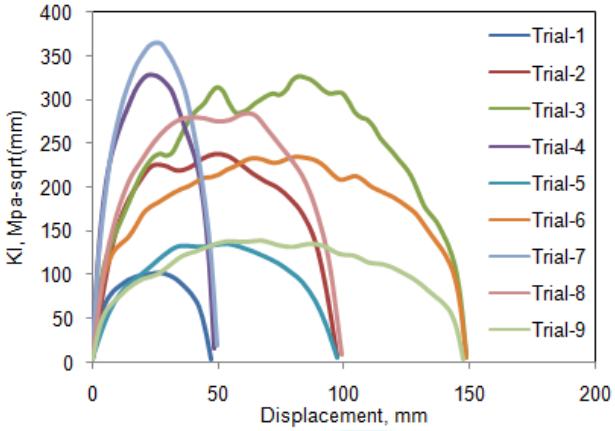

Figure 6: Stress intensity factors, KI of all test coupons.

3.5 Failure Criteria

The ANOVA summary of ultimate tensile strength (UTS) failure criterion is given in table 3. All parameters were accepted at 90% confidence level. The percent contribution indicates that the heat treatment of the pipes contributed 46.60% of the variation for the UTS criterion. The second major contribution (33.415) was of the crack length. The crack depth (C) and pipe thickness gave the same affect in the variation of the UTS criterion.

The effect of pipe thickness on the failure criteria is depicted in figure 7a. The failure of pipes increased with an increase in the crack length (figure 7). The failure was minimal for the pipes undergone the heat treatment T3 (figure 8). This was attributed to the hardness (Vickers) values of AA2090 pipes. The hardness (Vickers) values of T3, T84 and T83 heat treated pipes were, respectively, 97, 162 and 176. The increase in the hardness promotes brittle fracture in the pipes. The optimum conditions of test coupon 5 would satisfy the failure criterion (ES/UTS = 0.96275 <1.0) while all other conditions were failed to satisfy the failure criterion.

Table 3: ANOVA summary of the UTS failure criteria

Source	*Sum 1*	*Sum 2*	*Sum 3*	*SS*	*v*	*V*	*F*	*P*
A	10.51	8.53	8.31	0.49	2	0.245	208.20	9.60
B	8.07	7.57	11.72	1.7	2	0.85	722.33	33.41
C	8.42	8.38	10.55	0.51	2	0.255	216.70	9.99
D	6.50	13.60	27.36	2.37	2	1.185	1007.01	46.60
Error				0.01059	9	0.0012	1.00	0.40
T	33.50	38.08	57.94	5.08059	17			100

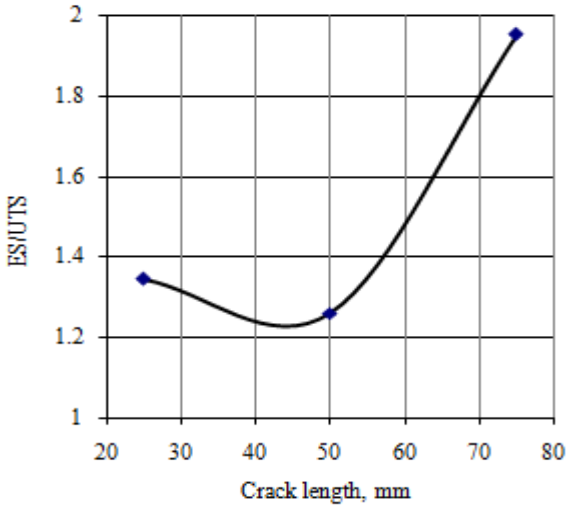

Figure 7: Effect of crack length on the failure criterion.

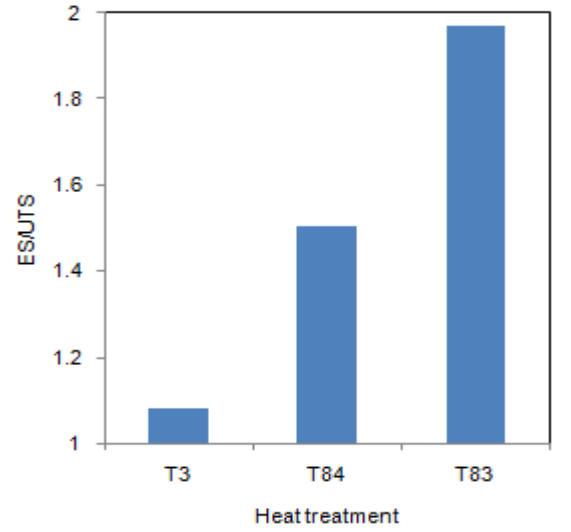

Figure 8: Effect of heat treatment on the failure criterion.

4. Conclusions

The failure of pipes increases with the increase of crack length. The failure of pipes under bursting pressure was low for the pipes heat treated with T3 conditions because of low hardness as compared to T83 and T84 heat treatments.

References

[1] American National Standards Institute (ANSI) / American Society of Mechanical Engineers (ASME): Manual for determining the remaining strength of corroded pipelines, ASME B31G, 1991.
[2] ANON; DNV-RP-F101, Corroded Pipelines, Det Norske Veritas, 1999.
[3] RITCHIE,D., LAST,S.; Burst Criteria of Corroded Pipelines - Defect Acceptance Criteria, Paper 32, Proceedings of the EPRG/PRC 10th Biennial Joint Technical Meeting on Line Pipe Research, Cambridge, UK, 18-21 April 1995, pp. 32-1 - 32-11.
[4] PRCI-Documents L51688B, A Modified Criterion for Evaluating the Remaining Strength of Corroded Pipe, 1989.
[5] A. Chennakesava Reddy, Evaluation of bursting pressure of thin walled 316 stainless steel tubes based on ASME B31G criterion, National Conference on Advances in Design Approaches and Production Technologies (ADAPT-2005), 22-23rd August 2005, Hyderabad, pp.225-228.
[6] A. Chennakesava Reddy, Evaluation of bursting pressure of thin walled 304 stainless steel tubes based on DNV RP F101criterion, National Conference on Advances in Design Approaches and Production Technologies (ADAPT-2005), 22-23rd August 2005, Hyderabad, pp.229-231.
[7] A. Chennakesava Reddy, Reliability assessment of corrosion in cold rolled 302 stainless steel tubes based on SHELL-92 criterion, National Conference on Advances in Design Approaches and Production Technologies (ADAPT-2005), 22-23rd August 2005, Hyderabad, pp.232-234.
[8] A. Chennakesava Reddy, Reliability assessment of corrosion in cold rolled 305 stainless steel tubes based on RSTRENG criterion, National Conference on Advances in Design Approaches and Production Technologies (ADAPT-2005), 22-23rd August 2005, Hyderabad, pp.235-237.
[9] D.U.M. Manikanta, A. Chennakesava Reddy, "Fracture Behavior of 6061 Al-Alloy Pipes under Bursting Loads with Crack Depth Variation," International Journal of Scientific & Engineering Research, Vol. 6, 338-343, 2015.
[10] D.U.M. Manikanta, A. Chennakesava Reddy, "Fracture Behavior of 6061 Al-Alloy Pipes under Bursting Loads with Crack Length Variation," International Journal of Advanced Research, ISSN: 2320-5407, Vol. 3, No. 4, pp. 657-665, 2015.
[11] D.U.M. Manikanta, A. Chennakesava Reddy, "Optimization of Fracture Behavior of AA6061 Al- Alloy Pipes Using Finite Element Analysis," International Journal of Science and Research, Vol. 4, pp. 1509-1515, 2015.
[12] C.R. Alavala, "CAD/CAM: Concepts and Applications," PHI Learning Pvt. Ltd., New Delhi, 2008.
[13] C.R. Alavala, "Finite element methods: Basic concepts and applications," PHI Learning Pvt. Ltd., New Delhi, 2008.
[14] J. Newman, I.S. Raju, "An Empirical Stress-Intensity Factor Equation for the Surface Crack," Engineering Fracture Mechanics vol.15, pp.185–192, 1981